Combinatorial screening of the effect of temperature on the microstructure and mobility of a high performance polythiophene semiconductor

Leah A. Lucas
Department of Chemical and Materials Engineering, Arizona State University, Tempe, Arizona 85284 and Flexible Display Center, Arizona State University, Tempe, Arizona 85284

Dean M. DeLongchamp,[a),b)] Brandon M. Vogel, Eric K. Lin, Michael J. Fasolka, and Daniel A. Fischer
Polymers Division, National Institute of Standards and Technology, Gaithersburg, Maryland 20899

Iain McCulloch and Martin Heeney
Merck Chemicals, Chilworth Science Park, Southampton S016 7QD, United Kingdom

Ghassan E. Jabbour[a),c)]
Department of Chemical and Materials Engineering, Arizona State University, Tempe, Arizona 85284 and Flexible Display Center, Arizona State University, Tempe, Arizona 85284

(Received 30 September 2006; accepted 30 October 2006; published online 4 January 2007)

Using a gradient combinatorial approach, the authors report the effects of temperature on the microstructure and hole mobility of poly(2,5-bis(3-dodecylthiophen-2yl)thieno[3,2-b]thiophene) thin films for application in organic field-effect transistors. The gradient heating revealed a detailed dependence on thermal history. Optimal heat treatment achieved mobilities as high as 0.3 $cm^2\ V^{-1}\ s^{-1}$. Mobility enhancement coincides with an increase in crystal domain size and orientation, all of which occur abruptly at a temperature closely corresponding to a bulk liquid crystal phase transition. © *2007 American Institute of Physics*. [DOI: 10.1063/1.2404934]

Polymer semiconductors require hole mobility similar to that of amorphous silicon to support organic field-effect transistors (OFETs) suitable for backplane active matrix liquid crystal display applications.[1] Recent synthetic approaches for polymer semiconductors have achieved facile solution processing, improved carrier mobility, and environmental stability.[2,3] With each of these improvements, it has become more clear that thin film microstructure critically influences performance. The microstructure controls the extent and organization of π-π stacking in the source-drain plane of an OFET, which is required for carrier transport.[4,5] The development of general methods to optimize microstructure remains a standing challenge because polymer semiconductors are sensitive to a wide variety of processing conditions. Casting solvent,[6,7] drying rate,[8] and thermal history all influence microstructure development. Combinatorial methods provide an excellent means to screen a wide parameter space by the use of continuous gradients to systematically and thoroughly probe processing conditions.[9,10]

We use a continuous combinatorial temperature gradient to evaluate the effect of temperature on the microstructure and mobility of a recently reported high performance polymer semiconductor, poly(2,5-bis(3-dodecylthiophen-2yl)thieno[3,2-b]thiophene) (pBTTT-C_{12}), shown in Fig. 1.[3] The pBTTT polymers, with varying alkyl side chain lengths, can achieve field-effect mobilities up to 0.6 $cm^2\ V^{-1}\ s^{-1}$ when heated to a liquid crystalline (LC) state and then cooled under nitrogen.[3] For pBTTT-C_{12}, mobilities up to 0.3 $cm^2\ V^{-1}\ s^{-1}$ were observed. In this previous work, heating to the LC state was accomplished at an arbitrary temperature well above the bulk LC phase transition without any detailed screening over a range of temperatures. A temperature gradient provides a systematic evaluation of the influence of thermal history on the thin polymer film, resulting in a smooth correlation of processing to polymer microstructure to OFET characteristics.

Top contact OFETs were fabricated on a common gate of highly *n*-doped silicon with a 200 nm thick thermally grown SiO_2 dielectric layer. The SiO_2 dielectric layer was modified with octyltrichlorosilane from a 2 mM solution in anhydrous hexadecane for 18 h at 25 °C. Films of pBTTT-C_{12} were spin coated at 3000 rpm ($3000\times 2\pi$ rad min^{-1}) from 5 mg ml^{-1} solutions in 1,2-dichlorobenzene heated to 100 °C in a nitrogen environment resulting in films that were 15 nm thick. Gold source and drain electrodes (100 nm thick) were evaporated and patterned through a shadow mask. OFETs were patterned in identical columns of five OFET geometries; channel width was either 1 or 2 mm and length varied from 80 to 220 μm. (Certain equipment, instruments, or materials are identified in this letter in order to adequately specify the experimental details. Such identification does not imply recommendation by the National Institute of Standards and Technology nor does it imply the materials are necessarily the best available for the purpose.) The ≈13 cm long substrate was patterned with 230 OFETs in

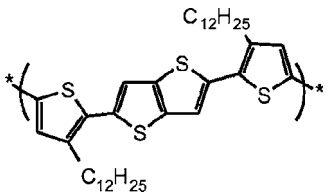

FIG. 1. Chemical structure of poly(2,5-bis(3-dodecylthiophen-2yl)thieno[3,2-b]thiophene) (pBTTT-C_{12}).

a)Authors to whom correspondence should be addressed.
b)Electronic mail: dean.delongchamp@nist.gov
c)Electronic mail: jabbour@asu.edu

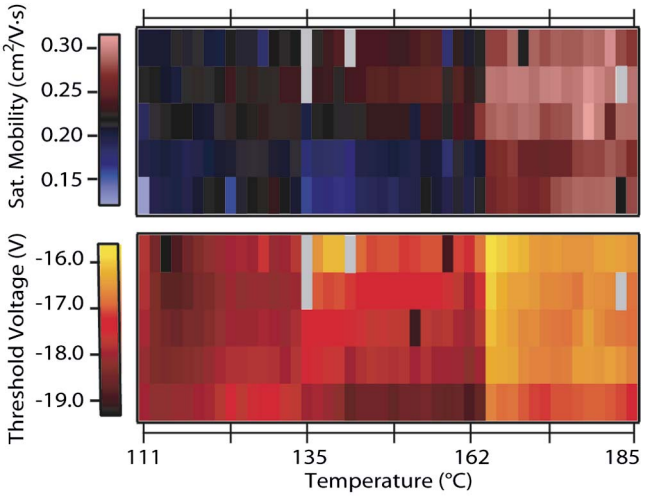

FIG. 2. (Color online) Field-effect saturation mobility (top) and threshold voltage (bottom) of pBTTT-C_{12} shown with respect to the temperature gradient. Each pixel represents an individual OFET. Gray pixels represent OFETs with excessive gate leakage. Standard error of the measurement is ≈3%. Device length (L) and width (W) dimensions (μm × mm) for the five OFETs in each column from top to bottom are 80 × 1, 105 × 1, 115 × 1, 120 × 2, and 221 × 2.

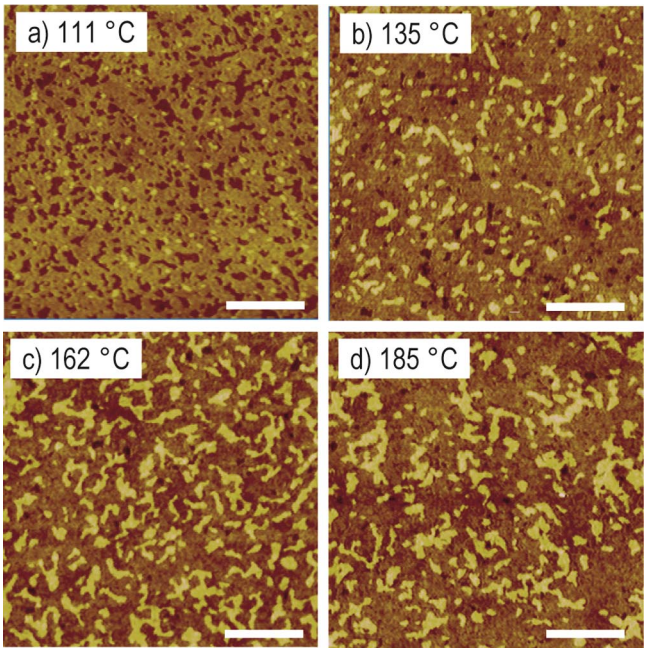

FIG. 3. (Color online) AFM topography images collected along the temperature gradient corresponding to the noted temperatures (°C). Vertical scale is 7 nm and scale bar is 500 nm.

closely spaced columns of 5, providing a resolution along the gradient of ≈3.5 OFET columns/cm.

The OFET substrate was heated on a thermal gradient stage in a nitrogen glovebox. One end of the stage was heated using a ceramic resistive element, and the other end was cooled using a flow of high-pressure nitrogen. The temperature of the gradient stage was calibrated using melting point standards (Reichert-Jung). This configuration can achieve a linear temperature gradient of $\Delta T \approx 90$ °C over 15.5 cm, providing a temperature resolution of one OFET column per ≈2 °C. For our experiments, the thermal gradient spanned from 111 to 185 °C. Once the temperature gradient stabilized, the OFET substrate was placed on the gradient stage for 5 min. Then the stage was allowed to cool until the highest temperature decreased from 185 to 80 °C, which required ≈15 min. For discrete samples, we have observed little or no variation in microstructure or mobility with cooling rate. The temperature gradient spans the crystalline and LC phases of pBTTT-C_{12}, as determined by differential scanning calorimetry (DSC).[3]

A programmable Cascade probe station was used for OFET characterization under a nitrogen environment. All OFETs displayed p-channel characteristics. The field-effect saturation mobility (μ_{sat}) and threshold voltage (V_T) of pBTTT-C_{12} were calculated from transfer curves using the following expression:

$$I_D = \frac{WC_i}{2L}\mu(V_G - V_T)^2, \quad (1)$$

where I_D is the saturation drain current, L the channel length, W the channel width, C_i the dielectric layer capacitance, V_G the gate voltage, and V_T the threshold voltage. The gradient heating of pBTTT-C_{12} films revealed the detailed dependence of mobility on thermal history. Figure 2 maps the field-effect saturation mobility (μ_{sat}) and threshold voltage (V_T) of the pBTTT-C_{12} film with respect to treatment temperature and transistor dimensions. Each pixel represents an individual OFET. Variation in mobility as a function of the channel length is not observed in pBTTT-C_{12} for these dimensions, but channel effects have been observed in lengths less than 50 μm. At temperatures less than 160 °C, the heating temperature does not influence mobility significantly. There is an abrupt transition between 160 and 165 °C, where the mobility increases from 0.20 to 0.27 $cm^2\ V^{-1}\ s^{-1}$ (uncertainty in mobility measurements is 0.01 $cm^2\ V^{-1}\ s^{-1}$). The mobility then plateaus again at higher temperatures. The highest mobility for a column of devices was at 179 °C, where the average mobility was 0.29 $cm^2\ V^{-1}\ s^{-1}$. This temperature also corresponds to the most positive threshold voltage column average value of −16.6 V. The threshold voltage also increased by 10% over the entire temperature range.

Atomic force microscopy (AFM) was used to image the surface morphology of the pBTTT-C_{12} OFET test bed at various points along the temperature gradient. Prior to heating, the as cast films had small nodule features and fibrils (not shown), which are similar to previous observations.[3] Terraces of ≈2 nm in height emerge at temperatures near the LC transition, as shown in Fig. 3. At the lowest temperature (111 °C), the terraces appear as small elliptical domains of diameter ≈33 nm [Fig. 3(a)]. As temperature increased, the terrace domain size also increased so that at the highest temperature (185 °C), the domains were ≈200 nm along their largest dimension [Fig. 3(d)]. The domains appear to coalesce or ripen with increased temperature. However, determination of the growth mechanism of the surface domains would require an *in situ* analysis of terrace evolution and is beyond the scope of this letter.

Orientational aspects of microstructure were evaluated using near edge x-ray absorption fine structure (NEXAFS) spectroscopy, which measures the absorption of soft x-rays into the resonant excitation of core 1s electrons to unfilled molecular orbitals.[11] A NEXAFS orientation analysis of the $1s \rightarrow \pi^*$ resonance near 285 eV provides the average tilt of the conjugated plane with respect to surface normal. The orientation of the conjugated plane can be characterized by a

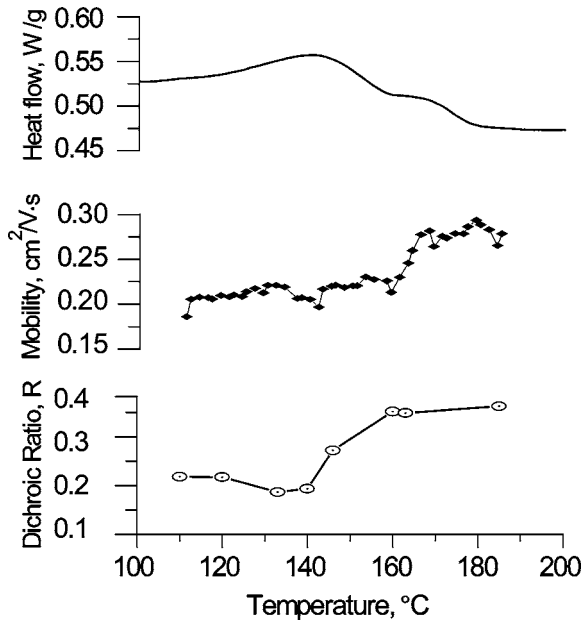

FIG. 4. (a) Differential scanning calorimetry of the pBTTT-C_{12}. The transition from crystalline solid to liquid crystal occurs at 150–160 °C. Standard error of measurement is ±1 °C. (b) Saturation mobility (shown as averaged values per column of OFETs mapped in Fig. 2) with respect to temperature gradient. (c) Dichroic ratio R calculated from NEXAFS spectra as a function of treatment temperature. Standard error of measurement is ≈1%.

dichroic ratio R, which varies from +0.7 for a fully vertical conjugated plane to −1.0 for a fully horizontal (flat) conjugated plane.[12] Figure 4(c) shows the R of pBTTT-C_{12} at various positions along the temperature gradient, calculated from NEXAFS spectra taken at five incident angles (20°, 33°, 44°, 55°, and 80°) for each position. At the low temperature end, $R \approx 0.22$, indicating a generally edge-on conjugated plane. The R increased at ≈145 °C and stabilized at 160 °C, in a more edge-on orientation with $R \approx 0.36$. The increase in apparent edge-on orientation is likely caused by a decrease in the disorder of the film, and not a change in its fundamental crystal structure. We note that the mobility appears to increase at temperatures somewhat higher than those required for structure improvement; future studies are underway to establish a greater point density for the NEXAFS orientation measurement and a comparison of other aspects of microstructure improvement such as crystallinity and side chain order.

The temperature gradient spans the crystalline to LC phase transition, as determined by DSC of bulk pBTTT-C_{12} [Fig. 4(a)]. The sharp increase in carrier mobility between 160 and 165 °C coincides with the heating of pBTTT-C_{12} into its LC phase [Fig. 4(b)]. Processing at any temperature within the LC phase region appears sufficient to increase the carrier mobility. Heating to temperatures above the LC transition does not further increase mobility or enhance order in the microstructure. Although one might expect differences in the thermal responses of the thin films used in OFETs versus the bulk powder analyzed by DSC, we find a good correlation between the powder phase transition and film mobility/microstructure improvement.

In summary, we use a combinatorial temperature gradient to develop a detailed correlation of processing to microstructure to performance for the high performance semiconducting polymer pBTTT-C_{12}. Mobility enhancement coincides with an increase in crystal domain size and orientation, all of which occur abruptly at a temperature closely corresponding to a bulk LC phase transition. The wide temperature window and fine resolution revealed details of the correlation that might have been missed in discrete samples. Additionally, the OFET gradient was prepared and processed on a single substrate, lowering potential sample-to-sample variation. This method may find general utility for screening OFET performance. This high-throughput approach can be used to optimize heat treatment, investigate materials with multiple phase transitions, or determine the lowest thermal budget required to increase performance.

The authors would like to acknowledge Dr. R. Joseph Kline for helpful discussions. One of the authors (L.A.L.) thanks the support of the Bell Labs Graduate Research Fellowship Program. Another author (B.M.V.) thanks the support of the NRC postdoctoral fellowship. This work was supported by the NIST Combinatorial Methods Center. Official contribution of the National Institute of Standards and Technology.

[1] G. Horowitz, J. Mater. Res. **19**, 1946 (2004).
[2] B. S. Ong, Y. Wu, P. Liu, and S. Gardner, J. Am. Chem. Soc. **126**, 3378 (2004).
[3] I. McCulloch, M. Heeney, C. Bailey, K. Genevicius, I. Macdonald, M. Shkunov, D. Sparrowe, S. Tierney, R. Wagner, W. Zhang, M. Chabinyc, R. J. Kline, M. McGehee, and M. Toney, Nat. Mater. **5**, 328 (2006).
[4] H. Sirringhaus, P. J. Brown, R. H. Friend, M. M. Nielsen, K. Bechgaard, B. M. W. Langeveld-Voss, A. J. H. Spiering, R. A. J. Janssen, E. W. Meijer, P. Herwig, and D. M. de Leeuw, Nature (London) **401**, 685 (1999).
[5] H. Sirringhaus, R. J. Willson, R. H. Friend, M. Inbasekaran, W. Wu, E. P. Woo, M. Grell, and D. D. C. Bradley, Appl. Phys. Lett. **77**, 406 (2000).
[6] M. J. Banach, R. H. Friend, and H. Sirringhaus, Macromolecules **37**, 6079 (2004).
[7] J.-F. Chang, B. Sun, D. W. Breiby, M. M. Nielsen, T. I. Solling, M. Giles, I. McCulloch, and H. Sirringhaus, Chem. Mater. **16**, 4772 (2004).
[8] D. M. DeLongchamp, B. M. Vogel, Y. Jung, M. C. Gurau, C. A. Richter, O. A. Kirillov, J. Obrzut, D. A. Fischer, S. Sambasivan, L. J. Richter, and E. K. Lin, Chem. Mater. **17**, 5610 (2005).
[9] T. X. Sun and G. E. Jabbour, MRS Bull. **27**, 309 (2002).
[10] G. Li and J. Shinar, Appl. Phys. Lett. **83**, 5359 (2003).
[11] J. Stohr, *NEXAFS Spectroscopy* (Springer, New York, 1996).
[12] D. DeLongchamp, E. Lin, and D. A. Fischer, Proc. SPIE **5940**, 59400A (2005).